

Optical investigations on indirect-band-gap $\text{Al}_x\text{Ga}_{1-x}\text{As}/\text{Al}_y\text{Ga}_{1-y}\text{As}$ superlattices

M.-E. Pistol, G. Paulsson, and L. Samuelson

Department of Solid State Physics, University of Lund, P.O. Box 118, S-221 00 Lund, Sweden

M. Rask and G. Landgren

Institute of Microwave Technology, P.O. Box 1084, S-164 21 Kista, Sweden

(Received 2 May 1988)

Indirect-band-gap, staggered $\text{Al}_{1-x}\text{Ga}_x\text{As}$ superlattices with two and three compositions have been grown by metal-organic vapor-phase epitaxy and studied with a variety of optical means, including photoluminescence, photoconductivity, and modulated-reflectance spectroscopy. Photoluminescence transitions involving charge carriers localized in different layers are observed. A value of 5.4–6.2 meV/at. % Al for the valence-band offset can be deduced from the photoluminescence measurements. Impurity-related emissions are demonstrated to be of importance in the photoluminescence spectra. Strong illumination induces shift of the Γ -band states of about 10 meV in the three-component superlattice, as detected by photoconductivity and electroreflectance. This effect which is similar to effects seen in doping superlattices, is shown to be strongly affected by a spacer layer of intermediate composition.

I. INTRODUCTION

The ability to epitaxially grow thin layers of semiconductors has opened a new field of physics and technology.¹ The best studied system is $\text{GaAs}/\text{Al}_{1-x}\text{Ga}_x\text{As}$ grown by molecular-beam epitaxy² or metal-organic vapor-phase epitaxy (MOVPE),³ where single quantum wells of GaAs ,⁴ as well as superlattices (SL),⁵ have been grown. Most of the studies have been reports dealing with direct-band-gap materials.^{6–8} Optical measurements on these systems are based mainly on photoluminescence (PL),⁹ photoluminescence-excitation (PLE) spectroscopy,¹⁰ and absorption¹¹ measurements. Only recently have the powerful techniques of modulated reflectance, such as electroreflectance (ER)¹² and photoreflectance,¹³ been used for the study of heterostructures. ER and PR probe the ground state as well as excited states of heterostructures and have been shown to have high sensitivity as well as high resolution when applied to heterostructures.¹⁴

We here report on optical studies, using PL, PLE, ER, and photoconductivity (PC), of $\text{Al}_{1-x}\text{Ga}_x\text{As}$ superlattices, where all layers are indirect-band-gap materials. Two superlattices were measured, one with two alloy compositions and one with three alloy compositions, to be described below.

PC and ER, performed with and without additional laser illumination, show that the band structure changes as a function of incident light. The shifts of the excited states with external illumination are discussed with reference to similar effects seen in doping superlattices.¹⁵ The PL results show that the superlattice is staggered, giving luminescence with an energy less than that of the band gaps of the constituent layers. The value of the valence-band slope as a function of composition is found to agree with previous PL studies of $\text{GaAs}/\text{Al}_{1-x}\text{Ga}_x\text{As}$ where

the alloy is an indirect-band-gap material^{6,7} and of $\text{GaAs}/\text{Al}_{1-x}\text{Ga}_x\text{As}$ made indirect by hydrostatic pressure.⁸

In Sec. II we will describe the experimental conditions including those of growth. In Sec. III we describe the results with special emphasis on the most important result of this study—the change in the band structure due to laser illumination. Finally, Sec. IV contains a summary and conclusions.

II. EXPERIMENTAL CONDITIONS

The superlattices were grown by MOVPE at atmospheric pressure, using TMAI , TMGa , and AsH_3 as precursors (where TM is trimethyl). The rf-heated reactor employs a horizontal quartz cell and was designed for abrupt interfaces and thickness uniformity, and has been described previously.¹⁶ The growth was continuous at 700 °C with 15 l/min of hydrogen-carrier-gas flow. The growth rate was 3 Å/min and the $[A^V]/[B^{III}]$ ratio was 50. Liquid-encapsulated Czochralski (LEC) grown GaAs wafers of (100) orientation were used as substrates. PL studies of single GaAs quantum wells in $\text{Al}_{1-x}\text{Ga}_x\text{As}$, grown in this system, show an excellent optical quality with PL linewidths of 6 meV (at 2 K) for well widths of 20 Å.¹⁷

The structure of the three-component sample, hereafter called sample 1, is shown in Fig. 1. A buffer layer of $\text{Al}_{0.6}\text{Ga}_{0.4}\text{As}$ was grown first and then the superlattice with layer thicknesses of 58 and 28 Å, as illustrated. final capping layers of $\text{Al}_{0.6}\text{Ga}_{0.4}\text{As}$ and GaAs completed the growth. The two-component sample, hereafter called sample 2, had exactly the same structure except that the 28 Å layers of $\text{Al}_{0.6}\text{Ga}_{0.4}\text{As}$ were absent. The average composition was determined by x-ray diffraction. A transparent gold film was evaporated onto the surface in

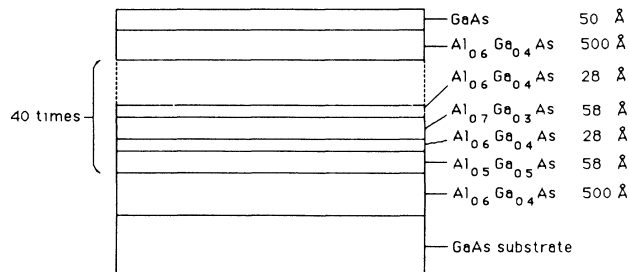


FIG. 1. The structure of sample 1 (not drawn to scale). The composition of the various layers and their thicknesses are given on the right. Sample 2 has the same structure but the 28-Å $\text{Al}_{0.6}\text{Ga}_{0.4}\text{As}$ layers are absent.

order to make a Schottky contact for the ER and PC experiments and Sn, Au, and Cr were alloyed through the structure to form an ohmic contact to the bottom buffer layer.

For the PL measurements the samples were immersed in pumped liquid helium at about 2 K and excited with the 5145-Å line of an Ar^+ -ion laser with a focused power of typically 20 mW. The emitted light was dispersed through a double monochromator, collected with a GaAs photomultiplier and subsequently amplified. A dye laser using Rhodamine-6G dye was used for the PLE measurements with the same detection system. The PLE spectrum was normalized with respect to the dye-laser intensity.

A halogen lamp and the monochromator were used for the reflectance measurements with a silicon *p-i-n* diode to detect the reflected light. A bias voltage of -0.5 V and an applied modulation voltage of 0.5 V were used for the ER measurements.

III. EXPERIMENTAL RESULTS

Figure 2 shows PL and ER spectra from sample 2. The PL signal is strong and has an energy which is 70 meV less than the band gap of the $\text{Al}_{0.5}\text{Ga}_{0.5}\text{As}$ layer. Previous PL measurements on bulk indirect-band-gap $\text{Al}_{1-x}\text{Ga}_x\text{As}$ grown under similar conditions showed no PL. We attribute this to impurity-related effects since the change in transition probability due to band folding¹⁸ is not expected to be strong in this sample due to the large superlattice period. Indeed, the separation of charges in this staggered SL should decrease the transition probability. The PL shape is unusual with a sharp high-energy cutoff similar to the M_0^x peak seen in indirect-band-gap $\text{GaAs}_{1-x}\text{P}_x$ ¹⁹ but dissimilar to the Gaussian line shape occurring in direct- and indirect-band-gap $\text{Al}_{1-x}\text{Ga}_x\text{As}$.^{20,21} However, an emission with this asymmetrical line shape has previously been predicted to occur in indirect $\text{Al}_{1-x}\text{Ga}_x\text{As}$.¹⁹ Curves (i) and (ii) show the PL at two different excitation intensities. It can be seen that the high-energy peak at about 617 nm and the band peaking at about 635 nm have different excitation-intensity dependences. This proves that the low-energy

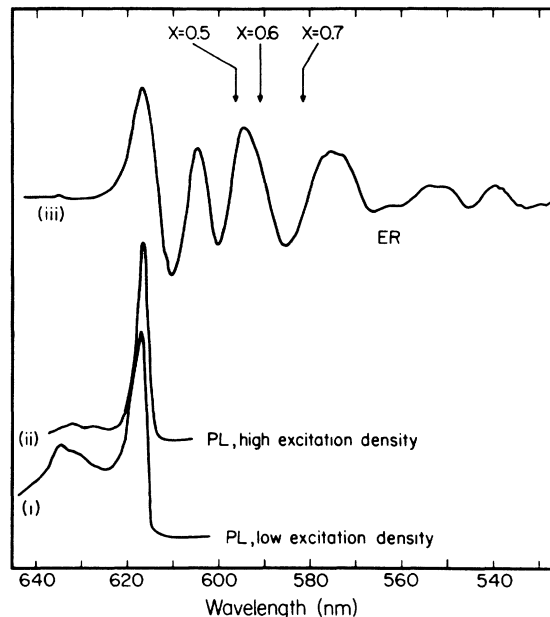


FIG. 2. Photoluminescence spectra and electroreflectance spectra of sample 2. The band gaps of the $\text{Al}_{1-x}\text{Ga}_x\text{As}$ layers in the sample are indicated by arrows. In this sample the electroreflectance starts at the same energy as the high-energy photoluminescence peak, thus indicating that this peak (at 617 nm) is not related to impurities but is a band-to-band transition, though possibly including excitonic effects. At lower excitation power the impurity-related PL emission at about 635 nm becomes more prominent.

band at 635 nm is not a phonon replica of the high-energy peak but more probably an impurity-related emission. The ER oscillations, curve (iii), start at the same energy as the high-energy PL peak, but no ER signal is seen from the impurity-related low-energy peak. Impurities are known to be able to cause ER,²² but the absence of ER in the impurity-related peak seen in PL indicates that the high-energy peak is a band-to-band transition, with possible excitonic contributions. The ER spectrum is remarkably strong considering that the SL is indirect in *k* space as well as in real space.

A valence-band offset of 5.4–6.2 meV/at. %Al can be calculated from the PL peak energy of sample 2, where the uncertainty is due to different values for the band gap versus composition, as found in the literature.^{23,24} For a recent recalibration of this function of the direct side see Ref. 21. We made use of Bastard's envelope-function approximation (EFA), as applied to direct-band-gap SL's, in calculating the superlattice minibands,²⁵ and assumed an exciton binding energy of 10 meV.²⁶ We used the valence-band offset as a parameter to fit the experiment. The use of EFA is not entirely justified here since there are three *X* valleys in each material that may interact. However, a more sophisticated treatment of the band structure in indirect Si/SiGe SL's, with the exception of a small splitting of the conduction band, gives very close agreement with the simple EFA.²⁷ A comparison between the calculated minibands and the ER spectrum is

not meaningful in this system since the X , L , and Γ bands are closely spaced, giving many possible transitions in the relevant spectral region.

Figure 3 shows PL, ER, PC, PLE, and resonantly excited PL of sample 1. The PL has a different shape than that for sample 2 but the sharp high-energy cutoff is similar. The PL emission was much weaker for this sample, which is not surprising since the charge carriers are more separated, as illustrated in Fig. 5. The ER spectrum, curve (ii), starts at a considerably higher energy in this sample showing that the absorption cross section for the lowest-energy transition is reduced, as expected, in com-

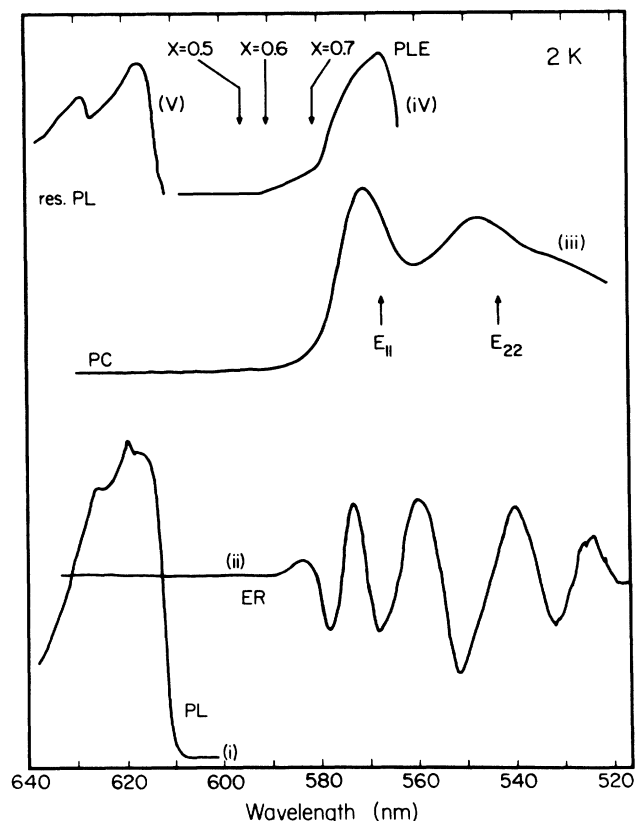


FIG. 3. A set of optical spectra from sample 1. The band gaps of the $\text{Al}_{1-x}\text{Ga}_x\text{As}$ layers in the sample are indicated by arrows. Curve (i) shows the photoluminescence and curve (ii) the electroreflectance spectrum. In contrast to sample 2, the electroreflectance spectrum starts at a considerably higher energy in this sample, showing the effect of the increased charge separation due to the extra spacer layer in this sample. Curve (iii) shows the photoconductivity spectrum. Curve (iv) shows the photoluminescence excitation spectrum which exhibits the same structure as the photoconductivity spectrum within the wavelength range of the dye. Selective excitation at 570 nm gives a somewhat different photoluminescence spectrum, curve (v), than the corresponding spectrum with excitation above the band gap, demonstrating that the photoluminescence band consists of several emissions. The calculated heavy-hole to Γ -band transition energies, E_{11} and E_{22} , are indicated by arrows for the two lowest-energy transitions, in good agreement with the states seen in photoconductivity.

parison with sample 1. PC measurements, curve (iii), show absorption starting at about the same energy as the ER oscillations. The PC shows two peaks, at 570 and 548 nm. Conventional oscillating PC²⁸ in the SL or the buffer layer cannot be the cause since the separation between the peaks (about 90 meV) is much larger than the LO phonon energy. A calculation of the energy levels, using the spacer-layer potential as a perturbation, gives absorption energies, indicated in Fig. 3, corresponding to transitions between the heavy hole and the ground state and the first-excited state of the Γ band. We thus ascribe the peaks to transitions involving heavy holes (first and second minibands) and the first and second minibands in the Γ band of the SL, and use the designations E_{11} and E_{22} . PLE, curve (iv), also shows a peak at 570 nm thus confirming that the corresponding peak seen in PC is not due to strong mobility variations of the states but rather to different absorption cross sections of the higher-lying SL states. Resonant excitation at 570 nm gives the PL shown by curve (v). The shape of the PL in this case is somewhat different from the PL obtained with above band-gap excitation, see curve (i). This proves that also in sample 2, the PL emission consists of at least two overlapping emissions. Resonant excitation at 620 nm did not give any detectable PL. Excitation-power-density variations also showed a change in the PL line shape. A small shift (4 meV) towards lower energy was seen at the lowest excitation density. Due to the uncertain cause of the PL emissions in this sample it was not clear if this was due to a change in the band gap or a change in the nature of the PL emission at different excitation power densities.

In order to further study possible optically pumped band-gap variations affecting the higher-energy transitions seen in PLE, PC, and ER, we performed PC and ER with and without laser excitation. The spectra obtained are displayed in Fig. 4. Application of external illumination consisting of about 20 mW of light with a wavelength of 363 nm from the laser, results in the peaks seen in PC being shifted about 10 meV towards higher energy. There are also changes in the ER spectrum. Due to the complexity of the ER signal the interpretation of these signal changes is not straightforward. However, in a more suitable SL, with larger separation of the minibands, ER has the advantage of higher resolution. A change in the built-in surface electric field produced by the photoexcited carriers is unlikely to be the cause of the shift since this would give a rather small shift in the opposite direction. We attribute the shifts to a light-induced change in the band structure, as illustrated in Fig. 5. When measuring PC without illumination the situation is as illustrated in Fig. 5(a), with only a few charge carriers in the SL, remembering that the light intensity in this case is only a few μW . With illumination consisting about 20 mW of uv light, charge carriers accumulate in their respective wells, the $x=0.7$ layers for electrons and the $x=0.5$ layers for holes. This effect, which is somewhat similar to the photopumping effect in doping superlattices,¹⁵ is illustrated in Fig. 5(b), and effectively causes an increase in the band gap of the SL. The subsequent increase in the barriers in the Γ band increases the energy levels of the Γ minibands, and it is this increase which is

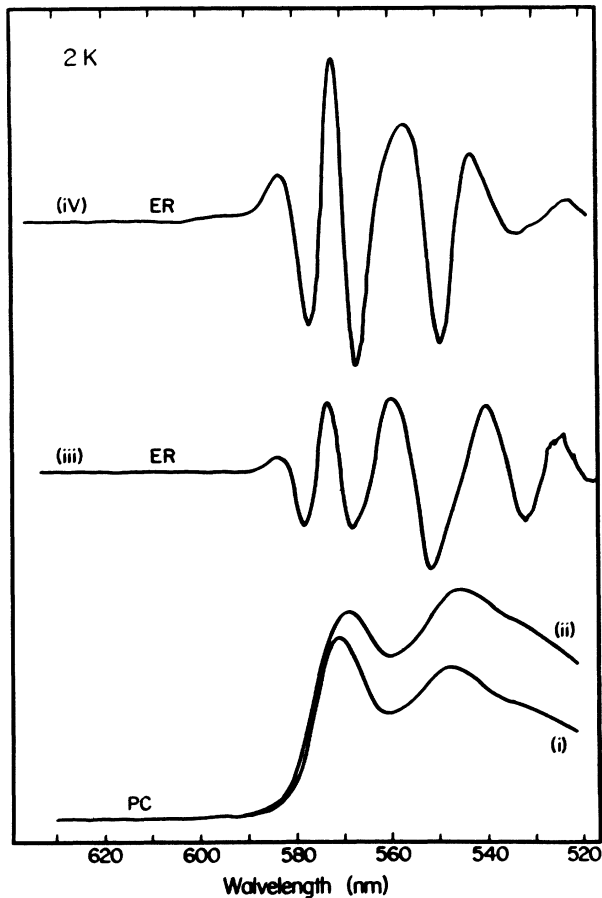


FIG. 4. The effect of additional laser illumination on sample 1. Curves (i) and (ii) show the shift of the photoconductivity when the sample is laser illuminated with curve (i) corresponding to no extra illumination. Curves (iii) and (iv) show the effect on the electroreflectance spectrum where curve (iii) is the "nonilluminated" spectrum.

seen in PC with laser illumination. Such effects were very weak in sample 2 demonstrating that the 28-Å $\text{Al}_{0.6}\text{Ga}_{0.4}\text{As}$ spacer layer is very important for this effect. Previous PL measurements on similar, staggered, two-component $\text{Al}_x\text{Ga}_{1-x}\text{As}/\text{Al}_y\text{Ga}_{1-y}\text{As}$ SL's with one layer being direct, showed no shift in the PL as a function of the excitation density,⁶ in agreement with our results. Due to the limited set of data we do not want to speculate about the role played by the spacer layer for this effect to occur.

Due to this change in the band structure with illumination, it is necessary to exercise caution when measuring band offsets in staggered superlattices by optical means such as PL. It is evidently necessary in PL measurements to go to very low-excitation densities and carefully check that the emission is a band-to-band emission.

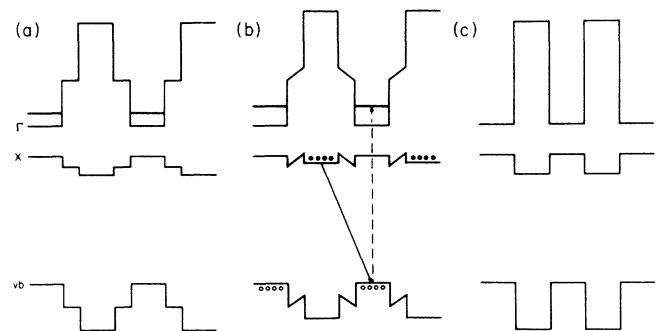


FIG. 5. The band structure of sample 1 without, (a), and with (b) illumination. The energy level of the lowest- Γ -band state is indicated (a) and (b). (a) Drawn to scale, except that the band gap has been decreased for clarity. The transitions seen in PL and PC are indicated by arrows, solid and dashed, respectively, (b). With illumination, the conduction-band wells (i.e., the $\text{Al}_{0.7}\text{Ga}_{0.3}\text{As}$ layers) become filled with electrons, filled circles, and the valence-band wells for holes (i.e., the $\text{Al}_{0.5}\text{Ga}_{0.5}\text{As}$ layers) become filled with holes, open circles. The electrostatic effects of the charge carriers will then give the approximate band structure (b). Note that the barriers for the Γ electrons increase causing an increase in their energies. The $\text{Al}_{0.6}\text{Ga}_{0.4}\text{As}$ spacer layer provides an extra separation between electrons and holes, compared with sample 2. (c) The band structure of sample 2 for comparison. In this sample the charge carriers are less separated.

IV. SUMMARY AND CONCLUSIONS

Using MOVPE we have grown indirect $\text{Al}_{1-x}\text{Ga}_x\text{As}$ superlattices with two and three compositions which have subsequently been studied with a variety of optical-spectroscopic methods. PL shows that the SL's are staggered and the value of the valence-band slope is found to be 5.4–6.2 meV/at.% Al. The strong PL signal shows that the SL quenches the nonradiative recombination in this system. ER shows quite a strong signal and a comparison of ER and PL shows that the absorption, as measured by ER, is strongly dependent on intermediate spacer layers in the SL. PC and PLE show that SL excited states in the Γ band can be measured in this system and that the excited states shift as a result of about 20 mW of external illumination with an argon-ion laser. This is interpreted as being the consequence of a change of the band structure, similar to the photoinduced change in band structure in doping superlattices. Impurity-related emissions are found to be important features of the PL emission in these indirect superlattices.

ACKNOWLEDGMENTS

This work was supported by grants from the National Swedish Board for Technical Development and by the Swedish Natural Science Research Council.

- ¹A. E. Blakeslee and C. F. Aliotta, *IBM J. Res. Dev.* **14**, 686 (1970).
- ²A. Y. Cho, *Appl. Phys. Lett.* **19**, 467 (1971).
- ³M. J. Ludowise, *J. Appl. Phys.* **58**, R31 (1985).
- ⁴P. M. Frijlink and J. Maluenda, *Jpn. J. Appl. Phys. Lett.* **21**, 574 (1982).
- ⁵A. Ishibashi, Y. Mori, M. Itabashi, and N. Watanabe, *J. Appl. Phys.* **58**(7), 2691 (1985).
- ⁶B. A. Wilson, P. Dawson, C. W. Tu, and R. C. Miller, *J. Vac. Sci. Technol. B* **4**, 1037 (1986).
- ⁷E. Finkman, M. D. Sturge, and M. C. Tamargo, *Appl. Phys. Lett.* **49**, 1299 (1986).
- ⁸D. J. Wolford, T. F. Kuech, T. W. Steiner, J. A. Bradley, M. A. Gell, D. Ninno, and M. Jaros, *Superlat. Microstructures* **4**, 525 (1988).
- ⁹R. C. Miller, D. A. Kleinman, W. A. Nordland, Jr., and A. C. Gossard, *Phys. Rev. B* **22**, 863 (1980).
- ¹⁰R. C. Miller, D. A. Kleinman, and A. C. Gossard, *Phys. Rev. B* **29**, 7085 (1984).
- ¹¹R. Dingle, W. Wiegmann, and C. H. Henry, *Phys. Rev. Lett.* **33**, 827 (1974).
- ¹²E. E. Mendez, L. L. Chang, G. Landgren, R. Ludeke, L. Esaki, and F. H. Pollak, *Phys. Rev. Lett.* **46**, 1230 (1981).
- ¹³B. V. Shanabrook, O. J. Glembocki, and W. T. Beard, *Phys. Rev. B* **35**, 2540 (1987).
- ¹⁴P. C. Klipstein, P. R. Tapster, N. Apsley, D. A. Anderson, M. S. Skolnick, T. M. Kerr, and K. Woodbridge, *J. Phys. C* **19**, 857 (1986).
- ¹⁵G. H. Döhler, G. Fasol, T. S. Low, J. N. Miller, and K. Ploog, *Solid State Commun.* **57**, 563 (1986).
- ¹⁶G. Landgren, S. G. Andersson, J. Y. Andersson, L. Samuelson, P. Silverberg, and P. Tolkien, *J. Cryst. Growth* **77**, 67 (1986).
- ¹⁷M.-E. Pistol, S. Nilsson, P. Silverberg, L. Samuelson, M. Rask, and G. Landgren, *Superlat. Microstructures* **2**, 501 (1986).
- ¹⁸U. Gnutzmann and K. Clauseker, *Appl. Phys.* **3**, 9 (1974).
- ¹⁹L. Samuelson, M.-E. Pistol, and S. Nilsson, *Phys. Rev. B* **33**, 8776 (1986).
- ²⁰E. F. Schubert, E. O. Göbel, Y. Horikoshi, K. Ploog, and H. J. Queisser, *Phys. Rev. B* **30**, 813 (1984).
- ²¹G. Oelgert, R. Schwabe, M. Heider, and B. Jacobs, *Semicond. Sci. Technol.* **2**, 468 (1987).
- ²²O. J. Glembocki, N. Bottka, and J. E. Furneaux, *J. Appl. Phys.* **57**, 432 (1985).
- ²³H. C. Casey and M. B. Duggan, *Heterostructure Lasers Part A* (Academic, New York, 1978).
- ²⁴R. Dingle, R. A. Logan, and J. R. Arthur, Jr., in *Gallium Arsenide and Related Compounds*, edited by C. Hilsum (Institute of Physics, London, 1977), p. 210.
- ²⁵G. Bastard, *Phys. Rev. B* **24**, 5693 (1981).
- ²⁶G. Duggan and H. L. Ralph, *Phys. Rev. B* **35**, 4512 (1987).
- ²⁷C. M. de Sterke and D. G. Hall, *Phys. Rev. B* **35**, 1380 (1987).
- ²⁸H. J. Stocker, and H. Kaplan, *Phys. Rev.* **150**, 619 (1966).